Conclusion

Our high-level calculations of the Diels-Alder reactions of aza- and phospha-1,3-butadienes reveal a number of interesting conclusions. Reasonable estimation of activation energies requires inclusion of electron correlation beyond the MP2 level. However, the TS geometry is little affected by correlation.

Geometric and density analysis based on the "progress ratio" of reactions 2-7 indicate that these reactions are asynchronous. However, estimates of the bond orders in the TSs suggest that these reactions are synchronous. Further study on this issue is clearly needed to determine the errors and biases imposed by these two methods. However, direct analysis of the electron density in the TS may prove to be more appropriate for understanding the bonding changes that occur in a reaction. For these systems, such an analysis argues for synchronous reactions.

The difficulty in having 1-aza-1,3-butadienes undergo DA reactions can be attributed to two energetic factors. First, the DA reactions of 2 and 3 are less exothermic than the prototype DA reaction. Second, the activation energy of these reactions is quite large, which is attributable to a low-lying HOMO. Thus, Boger's recent development of inverse electron demand DA methodology, taking advantage of the low LUMO, is quite appropriate.[15,16] The success of FMO theory in predicting the relative ordering of the activation energies of the reactions further supports the notion of extending this mechanistic theory from hydrocarbon systems to heteroatomic systems.

The energetics of DA reactions of phosphabutadienes are quite favorable. The activation energy of reactions 5-7 are small, less than 20 kcal mol^{-1} for 1-phospha-1,3-butadiene and 28 kcal mol^{-1} for 2-phospha-1,3-butadiene. These reactions are strongly exothermic. These calculated energies are completely consistent with the albeit scant available synthetic literature. Phosphabutadienes with small substituents readily undergo [4 + 2] self-addition and the isolated diene is not observed.[1,2]

On the other hand, phosphabutadienes with large substituents can be isolated and they do not react as dienes in cycloaddition reactions.[1] These calculations indicate that there is no large barrier or unfavorable reaction energy for the DA reaction of phosphabutadienes. Our previous study of the rotational barrier of phosphabutadienes revealed only normal energy barriers between the s-trans and s-gauche conformers.[9] However, bulky substituents will increase this barrier and disfavor the s-cis conformer. Phosphabutadienes contained within a ring, and thus restricted to the s-cis conformation, readily undergo DA chemistry.[8] The inability of the heavily substituted acyclic phosphabutadienes to access the s-cis conformation appears to be the only reasonable explanation for their inability to act as the diene fragment of the DA reaction. Balancing the need to preclude the self-DA reaction while still allowing access to the s-cis conformation for other DA chemistry on the basis of steric alone appears to be self-defeating, outside of restricting the diene to be in a ring.

Acknowledgment is made to the Donors of the Petroleum Research Fund, administered by the American Chemical Society, and the National Science Foundation for partial support of this research.

Supplementary Material Available: Optimized geometries in the form of Z Matrices for structures 8-19 at the HF/6-31G* and MP2/6-31G levels (12 pages). This material is contained in many libraries on microfiche, immediately follows this article in the microfilm version of the journal, and can be ordered from the ACS; see any current masthead page for ordering information.

Molecular Recognition through C-H•••O Hydrogen Bonding in Charge-Transfer Crystals: Highly Selective Complexation of 2,4,7-Trinitrofluorenone with 2,6-Dimethylnaphthalene

Takanori Suzuki, Hiroshi Fujii,† and Tsutomu Miyashi*

Department of Chemistry, Faculty of Science, Tohoku University, Sendai 980, Japan

Yoshiro Yamashita

Institute for Molecular Science, Okazaki 444, Japan

Received May 15, 1992

Treatment of a dimethylnaphthalene (DMN) isomer mixture with 2,4,7-trinitrofluorenone (TNF) resulted in the predominant formation of 2,6-DMN·TNF (1:1) complex (3) accompanied by a small amount of 2,7-DMN·TNF (1:1) (4). X-ray structural analyses of these charge-transfer crystals showed that coplanar "ribbon"-like networks are formed by C-H···O hydrogen bonding of TNF and that 3 is thermodynamically more stable than 4 due to the larger interactions through C-H···O contacts.

Hydrogen bonding through the short C-H···O contacts in crystals has been known to play a significant role in determining the molecular packing of organic solids.[1-3] This weak bonding has proven effective in steering flat molecules into the adoption of layered crystal structures,[4,5] and an electrostatic stabilization of at least 1.8 kcal mol^{-1} was estimated experimentally.[6] On the other hand,

† On leave from Mitsubishi Oil Co., Ltd., Research Laboratory for Development, 4-1, Ohgimachi, Kawasaki-ku, Kawasaki, 210 Japan.

(1) Taylor, R.; Kennard, O. *J. Am. Chem. Soc.* **1982**, *104*, 5063. It was reported that C-H groups which are adjacent to nitrogen atoms are particularly likely to participate in this bonding.
(2) Desiraju, G. R. *Acc. Chem. Res.* **1991**, *24*, 290.
(3) Typical values for the H···O and C···O distances are 2.4-3.0 Å (ref 1) and 3.3-3.8 Å (ref 2), respectively, in C-H···O hydrogen bonding.

0022-3263/92/1957-6744$03.00/0

crystalline charge-transfer complexes (CT crystals) of polynitro compounds such as picric acid and 2,4,7-trinitrofluorenone (TNF) have been used for the identification and separation of organic hydrocarbons.[7] Because the oxygen atoms of nitro groups are good hydrogen acceptors in C-H···O bonding,[5] molecular arrangements in these complexes may be affected by this weak bonding. CT interactions from hydrocarbon donors to polynitro acceptors will enforce C-H···O bonding by increasing both the acidity of the hydrogens[2] and the negative charge on the nitro groups. We have found that the complexation of TNF with a mixture of dimethylnaphthalene (DMN) isomers exhibited a high 2,6 isomer selectivity. It is intriguing that TNF was able to distinguish 2,6-DMN (1) from 2,7-DMN (2) in light of the fact that 1 and 2 possess such similar molecular shapes that a eutectic mixture was formed on crystallization. We report herein the importance of the role of C-H···O hydrogen bonding in TNF, leading to the differentiation of DMN isomers.

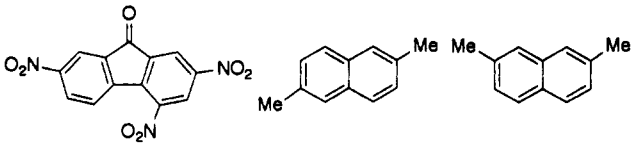

TNF 2,6-DMN (1) 2,7-DMN (2)

2,6-DMN·TNF (1:1) CT crystal : (3)

2,7-DMN·TNF (1:1) CT crystal : (4)

Result

Complexation of TNF with DMNs. By suspending finely powdered TNF (E^{red} −0.48 V) in a DMN mixture containing 8.3 wt % of 1 (E^{ox} +1.46 V) and 8.1 wt % of 2 (E^{ox} +1.52 V) for 36 h at 20 °C, orange CT crystals were obtained in 59% yield. Thermal decomplexation of the CT crystals under reduced pressure gave colorless crystals substantially enriched in 1 (1, 87.9 wt %; 2, 5.6 wt %), and TNF was recovered quantitatively. This procedure resulted in a 10-fold concentration of 1 whereas the concentration of 2 was reduced to two-third of its initial value. By repeating the process, even further concentration of 1 could be achieved (99.91 wt %). These results indicate that TNF was able to distinguish 1 from 2 or other isomers during the complexation, and the procedure described above can be applied to the separation of 1 from a DMN isomer mixture.

The association constants (K_{CT}) for the electron donor–acceptor complexes were the same for 1–TNF and 2–TNF (1.3 mol^{-1} dm^3 at 30 °C and 2.8 mol^{-1} dm^3 at 0 °C in CH_2Cl_2), indicating that molecular recognition by TNF does not occur in solution[8] but rather in the crystal formation step. Furthermore, the observed selectivity for 1 was dependent on the reaction time for complexation (Figure 1). Thus, initially formed CT crystals of low selectivity gradually gave way to those containing mainly 1 after 30 h. Efficient stirring was necessary in order to achieve the equilibrium for high selectivity; recrystallization of TNF from a DMN mixture followed by maintenance at room temperature for 72 h afforded the CT crystals of various isomers (1, 6.6 wt %; 2, 7.9 wt %). These results clearly show that the observed high selectivity can be explained in terms of greater thermodynamic stability for the CT crystal of 2,6-DMN·TNF (1:1) (3) than for 2,7-DMN·TNF (1:1) (4) or those of other isomers. In order to further investigate the factors contributing to the different thermodynamic stabilities in CT crystals, structural analyses of 3 and 4 were carried out.

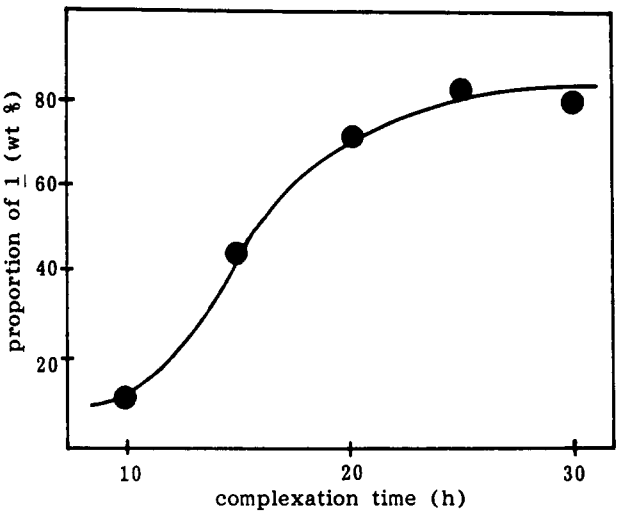

Figure 1. Reaction time dependence of 2,6-DMN selectivity. Proportion of 1 in the DMN obtained by thermal decomplexation of CT crystals is plotted as a function of complexation time of TNF with a DMN mixture at 20 °C.

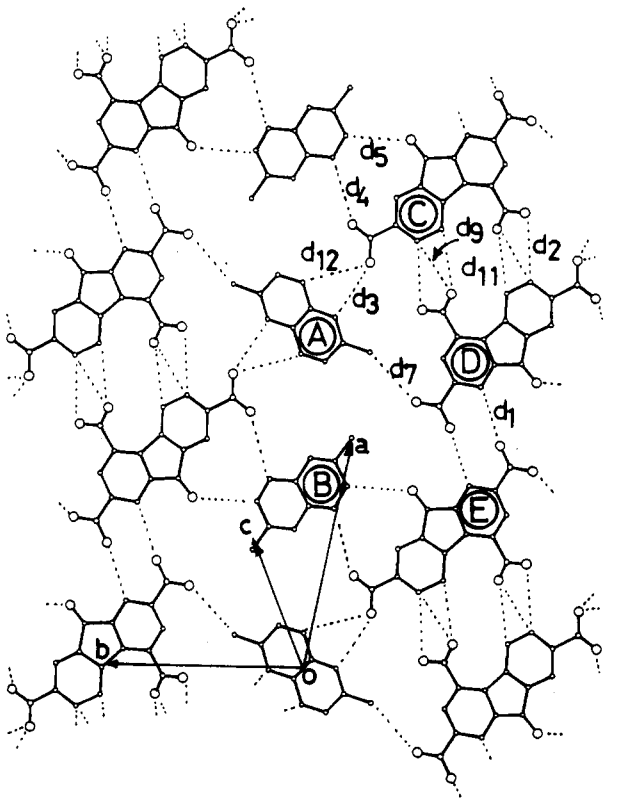

Figure 2. Nearly coplanar arrangement of molecules in 3. Hydrogen atoms are omitted for clarity. Two crystallographically independent molecules of 1 (A and B on the center of symmetry) are aligned along the [101] direction. C···O contacts in C-H···O bonding (d_1, d_2, d_3, d_4, d_5, d_7, d_9, d_{11}, and d_{12}) are shown by dotted lines, and the distances and angles are given in Table I. Interplanar deviations between two molecular planes are as follows: 1.18 Å for A and C, 0.08 Å for A and D, 1.16 Å for B and D, 0.75 Å for B and E, 0.63 Å for C and D, and 0.72 Å for D and E.

(4) Desiraju, G. R. *Acc. Chem. Res.* **1986**, *19*, 222.
(5) Sarma, J. A. R. P.; Desiraju, G. R. *J. Chem. Soc., Perkin Trans. 2* **1987**, 1195.
(6) Seiler, P.; Dunitz, J. D. *Helv. Chem. Acta* **1989**, *72*, 1125.
(7) Foster, R. In *Organic Charge-Transfer Complex*; Academic Press: London and New York, 1969; pp 379–390.
(8) Cooper, A. R.; Crowne, C. W. P.; Farrell, P. G. *Trans. Faraday Soc.* **1967**, *63*, 447.

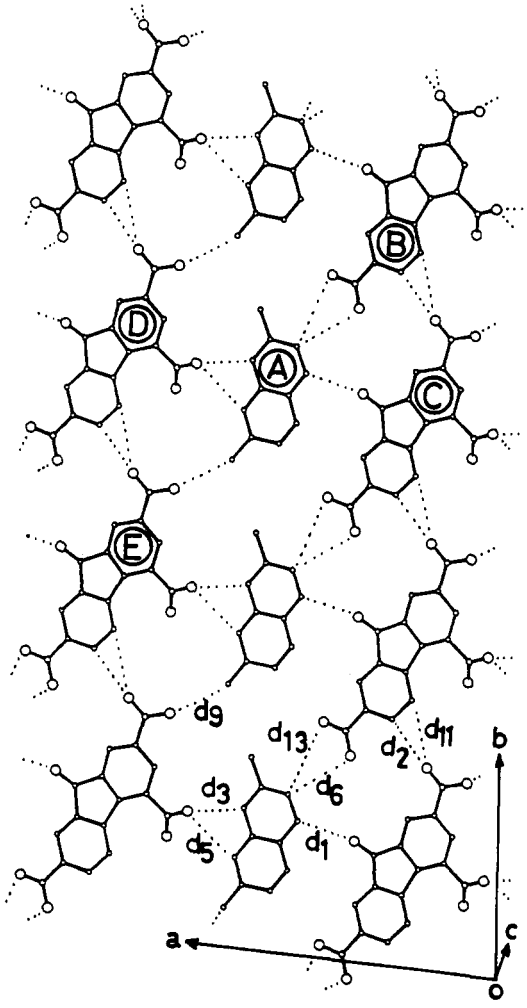

Figure 3. Nearly coplanar arrangement of molecules in **4**. Hydrogen atoms are omitted for clarity. TNF and **2** are aligned along the *b* axis. No transposition of methyl groups was observed. C···O contacts in C–H···O bonding (d_1, d_2, d_3, d_5, d_6, d_9, d_{11}, and d_{13}) are shown by dotted lines, and the distances and angles are given in Table II. Interplanar deviations between two molecular planes are as follows: 0.33 Å for A and B, 1.31 Å for A and C, 1.73 Å for A and D, 0.08 Å for A and E, and 0.74 Å for B and C.

X-ray Structural Analyses. In the crystal of **3**, several of the C–H···O atomic contacts are shorter than the sum of the van der Waals (vdW) radii (2.6 Å)[9] as shown in Table I.[3] TNF molecules related by a center of symmetry are connected to each other by several kinds of C–H···O bonding, resulting in the formation of nearly coplanar "ribbon" networks along the [101] direction (Figure 2). Spatial cavities are formed between the two "ribbons" nearly on the same plane. Each of two crystallographically independent molecules of **1** (A and B) is incorporated in the center of the cave and aligned alternately in order to prevent unfavorable contacts with the prominent nitro groups. These structural features indicate that this crystal can be regarded as belonging to the host–guest type and that TNF forms linear and coplanar lattices through C–H···O bonding. It is noteworthy that C–H···O contacts are also observed between **1** and TNF in the lateral direction which may also stabilize the crystalline state of **3**.

Similar coplanar "ribbon" networks were also observed in the crystal of **4**. However, the network seems looser in **4** than in **3**, and the connected TNF molecules are related by unit translations along the *b* axis (Figure 3). Molecules of **2** are also aligned along the *b* axis and incorporated between the two "ribbons" exhibiting C–H···O contacts with TNF (Table II). These results indicate that this crystal is also of the host–guest type, although the stabilization through C–H···O bonding seems smaller than in **3**.

Perpendicular to the molecular planes, one-dimensional mixed stacks of DMN and TNF were formed in both **3** and

(9) Pauling, L. In *The Nature of Chemical Bond*, 3rd ed; Cornell University Press: Ithaca, NY, 1960; pp 260, Tables 7–20.

Table I. Interatomic Distances (d) and Angles (θ) for C–H•••O Bonding in 3[a]

contact[b]	d(H···O)	d(C···O)	θ(C–H···O)	direction
d_1:C(1)–H(1)···O(21)	2.36	3.32	147.0	lateral
d_2:C(6)–H(6)···O(41)	2.43	3.49	167.0	lateral
d_3:C(31)–H(31)···O(71)	2.43	3.39	159.5	lateral
d_4:C(44)–H(44)···O(72)	2.55	3.59	153.2	lateral
d_5:C(43)–H(43)···O(9)	2.60	3.62	166.2	lateral
d_6:C(36)–H(362)···O(41)	2.71	3.40	127.3	stack
d_7:C(36)–H(361)···O(22)	2.78	3.49	127.5	lateral
d_8:C(46)–H(462)···O(21)	2.84	3.71	141.3	stack
d_9:C(6)–H(6)···O(42)	2.87	3.55	121.2	lateral
d_{10}:C(46)–H(462)···O(22)	2.88	3.46	115.5	stack
d_{11}:C(5)–H(5)···O(42)	2.89	3.53	120.0	lateral
d_{12}:C(34)–H(34)···O(71)	2.94	3.78	139.5	lateral
d_{13}:C(36)–H(363)···O(9)	2.94	3.57	124.1	stack
d_{14}:C(44)–H(44)···O(21)	2.97	3.83	132.9	stack[c]
d_{15}:C(34)–H(34)···O(42)	2.97	3.65	123.4	stack[d]

[a] Distances in angstroms and angles in degrees. The contacts with d(H···O) < 3.0, d(C···O) < 4.0, and θ(C–H···O) > 110° were accepted as C–H···O bonding. [b] Each of C–H···O contacts was assigned by d number in order to indicate the connected molecules in the crystal in Figures 2 and 4. [c] The contact between TNF (molecule D) and **1** (overlapped with molecule E) in Figure 2. [d] The contact between TNF (molecule D) and **1** (overlapped with molecule C) in Figure 2.

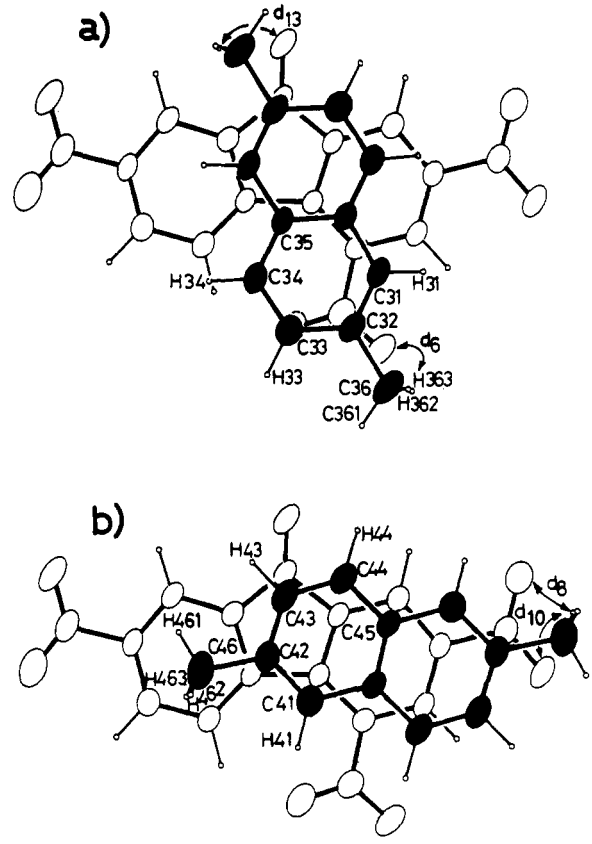

Figure 4. Molecular overlapping of TNF and **1** [molecule A in a and B in b] in **3** viewed perpendicularly to the molecular plane of TNF. The interplanar distances and dihedral angles are 3.46 Å and 2.0° in the former, and 3.40 Å and 3.4° in the latter, respectively. C–H···O contacts (d_6, d_8, d_{10}, and d_{13}) are shown by arrows, and the distances and angles are given in Table I. Each of molecules A and B exists on the center of symmetry and their atom numbering systems are shown. Numbering of TNF is the same as shown in Figure 5b.

Table II. Interatomic Distances (d) and Angles (θ) for C-H•••O Bonding in 4[a]

contact[b]	d(H···O)	d(C···O)	θ(C-H···O)	direction
d_1:C(34)-H(34)···O(9)	2.38	3.30	156.5	lateral
d_2:C(6)-H(6)···O(21)	2.46	3.23	131.4	lateral
d_3:C(31)-H(31)···O(41)	2.62	3.44	132.9	lateral
d_4:C(41)-H(412)···O(42)	2.67	3.50	146.5	stack
d_5:C(38)-H(38)···O(41)	2.67	3.53	136.3	lateral
d_6:C(33)-H(33)···O(71)	2.73	3.77	162.1	lateral
d_7:C(42)-H(422)···O(21)	2.73	3.67	145.6	stack
d_8:C(42)-H(422)···O(22)	2.78	3.55	127.8	stack
d_9:C(42)-H(421)···O(22)	2.78	3.32	115.4	lateral
d_{10}:C(3)-H(3)···O(42)	2.88	3.84	149.0	stack[c]
d_{11}:C(5)-H(5)···O(21)	2.89	3.48	115.6	lateral
d_{12}:C(42)-H(423)···O(22)	2.90	3.54	120.4	stack
d_{13}:C(33)-H(33)···O(72)	2.91	3.90	151.8	lateral
d_{14}:C(41)-H(411)···O(21)	2.97	3.54	131.8	stack[d]

[a] Distances in angstroms and angles in degrees. The contacts with d(H···O) < 3.0, d(C···O) < 4.0, and θ(C-H···O) > 110° were accepted as C-H···O bonding. [b] Each of C-H···O contacts was assigned by d number in order to indicate the connected molecules in the crystal in Figures 3 and 5. [c] The contact between TNF (molecule D) and TNF (overlapped with molecule A) in Figure 3. [d] The contact between TNF (molecule C) and 2 (overlapped with molecule B) in Figure 3.

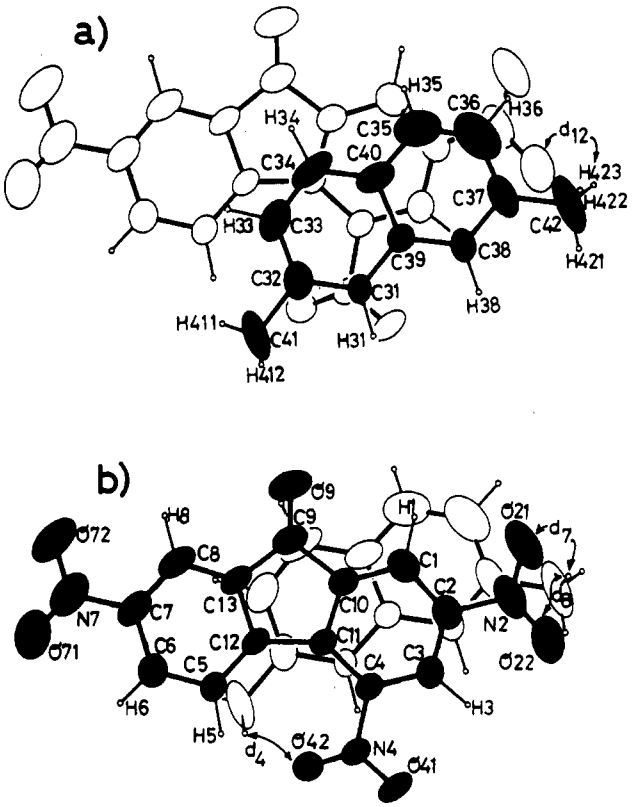

Figure 5. Two types of molecular overlapping of 2 and TNF in 4 [2 (x, y, z), TNF (1-x, 1-y, -z) in a; 2 (x, y, z), TNF (1-x, 1-y, 1-z) in b] viewed perpendicularly to the molecular plane of TNF. The interplanar distances and dihedral angles are 3.39 Å and 4.5° in the former, and 3.36 Å and 4.5° in the latter, respectively. C-H···O contacts (d_4, d_7, d_8, and d_{12}) are shown by arrows, and the distances and angles are given in Table II. Atom numbering systems of 2 and TNF are shown in a and b, respectively.

4. These mixed stacks are quite common packing arrangements in CT crystals of planar molecules. There exist several C-H···O contacts through the face-to-face overlappings of TNF and 1 or 2 (Figures 4 and 5) although the distances are rather longer than those in the lateral directions.

Discussion

The present work has revealed that polynitro acceptors like TNF can form spatial cavities through C-H···O hydrogen bonding in CT crystals. This weak bonding leads to layered crystal structures and coplanar "ribbon" networks of TNF in both 3 and 4. However, the molecular arrangements in the "ribbons" of the two crystals are dissimilar because of the different molecular symmetries of 1 (C_{2h}) and 2 (C_{2v}). Each of two crystallographically independent molecules of 1 exist on a center of symmetry in 3, such that the surrounding TNF molecules are related by inversion centers. Thus, the TNF molecules in 3 are connected in head-to-head and tail-to-tail manners, similar to the case of TNF itself.[10] On the other hand, all the molecules in a layered structure in 4 are related by unit translations rather than inversion centers, and the connected TNF molecules are aligned in the head-to-tail fashion. Because of these differences in packing arrangements, C-H···O bonding patterns in 3 and 4 are dramatically different, as shown by a comparison of scattering plots of O···H distances vs C-H···O angles (θ)[11] (Figure 6). On first inspection, C-H···O bonding in 3 can

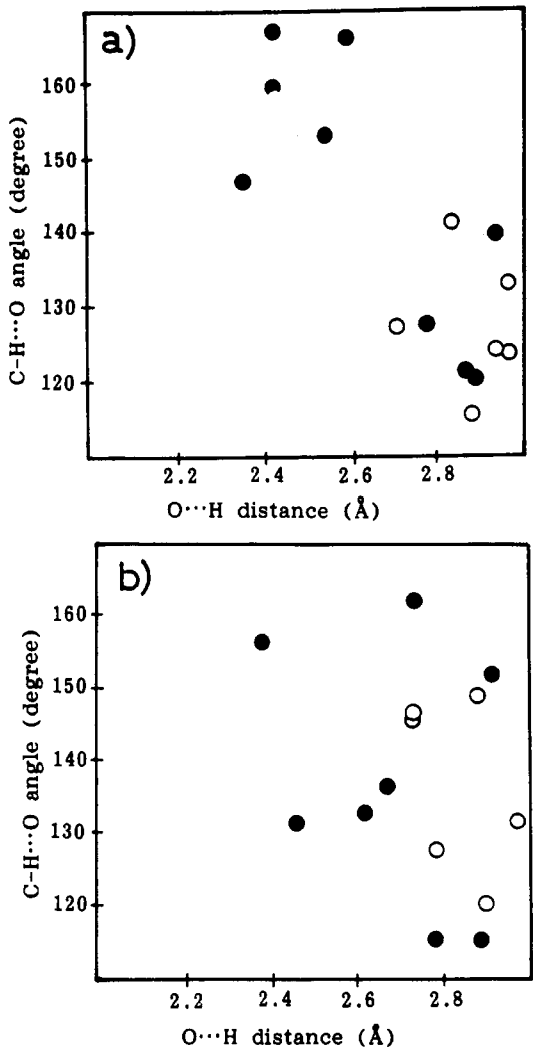

Figure 6. Scattering plots of O···H distances vs C-H···O angles of C-H···O bonding in 3 (a) and 4 (b). The contacts where C···O < 4.0 Å, O···H < 3.0 Å, and C-H···O > 110° were accepted as C-H···O bonding. The contacts through the face-to-face overlappings are shown by open circles, and the filled circles indicate those in the lateral directions. Please note the two distinct clusters in a but no remarkable cluster in b.

(10) Doeset, D. L.; Hybl, A.; Ammon, H. L. *Acta Crystallogr. Sect. B* 1972, *28*, 3122.

(11) The C-H···O hydrogen bonding shows relatively fixed angular geometries of θ (150-160°) (ref 2). Thus, the contacts with smaller θ values may be less important in stabilizing the crystalline state.

be classified into two groups, the "stronger" bond with a shorter length (ca. 2.5 Å) and good linearity (θ 150–170°) and the "weaker" bond with a longer length (ca. 2.8 Å) and an angle in the range of 120–140° (Figure 6a). The five contacts in the lateral directions were assigned as "stronger" and should play a significant role in stabilizing the crystalline state of 3. On the other hand, distribution of C–H···O bonding in 4 did not show remarkable cluster in the scattering plot (Figure 6b), and only one contact can be classified as a "stronger" C–H···O bond in a sense similar to that of 3. Although thermodynamic stability in the crystalline states of 3 and 4 is affected by a complex blend of electrostatic, van der Waals, and stacking forces, stabilization by C–H···O bonding is the most likely explanation for the observed discrimination of 1 from 2 by TNF in a crystal.

Experimental Section

General. Melting points are uncorrected. GC analyses were carried out by using a 50 m capillary column of DMN267.

Complexation of TNF with a DMN Isomer Mixture and the Successive Thermal Decomplexation of the CT Crystals. The mixture used for the complexation is a fraction obtained at the catalytic reforming petroleum oil having a boiling point of 250–270 °C. This material contains DMN isomers in the following ratio: 2,6-DMN (1), 8.34 wt %; 2,7-DMN (2), 8.10 wt %; 1,6-DMN, 7.93 wt %; 1,2-, 1,3-, and 1,4-DMN, 15.20 wt %; 1,5- and 1,7-DMN, 9.07 wt %; 1,8-DMN, 2.62 wt %; 2,3-DMN, 3.60 wt %; other aromatic hydrocarbons (naphthalene, methylnaphthalenes, ethylnaphthalenes, and biphenyl), 17.20 wt %; nonaromatic hydrocarbons, 27.94 wt %. Powdered TNF (4.00 g, 12.7 mmol) was dissolved in 67.6 g of the DMN mixture (1; 5.61 g, 36.0 mmol) and stirred for 36 h at 20 °C. Orange precipitates were gradually formed on stirring which were collected by suction, washed with *n*-hexane (5 mL × 5), and dried in vacuo (10^{-2} Torr, 6 h), giving 3.54 g of CT crystals in 59% yield based on TNF and an assumed 1:1 ratio of TNF and DMN, mp 140–150 °C dec. The resulting CT crystals (2.84 g, 6.04 mmol) were heated at 120–140 °C under 19 Torr by using a Kugelrohr glass tube oven, giving 1.90 g (100%) of TNF as a yellow powder and 912 mg of colorless crystals. GC analysis of the hydrocarbon fraction showed that 1 was enriched substantially (1, 87.86 wt %; 2, 5.63 wt %; 1,6-DMN, 1.99 wt %; 1,2-, 1,3-, and 1,4-DMN, 0.72 wt %; 1,5- and 1,7-DMN, 0.41 wt %; 1,8-DMN, 0.40 wt %; 2,3-DMN, 1.37 wt %; 2-methylnaphthalene, 1.26 wt %; 2-ethylnaphthalene and biphenyl, 0.37 wt %).

The hydrocarbon obtained above (912 mg; 1, 87.86 wt %; 2, 5.63 wt %) was dissolved in 8.88 g of toluene, and the concentration of 1 was adjusted to 8.28 wt %. Powdered TNF (571 mg, 1.81 mmol) was added, and the whole mixture was stirred for 38 h at 20 °C. Separated orange precipitates were filtrated, washed with *n*-hexane (1 mL × 5), and dried in vacuo (10^{-2} Torr, 7 h), giving 760 mg of CT crystals in 89% yield based on TNF, mp 153–155 °C dec. CT crystals thus obtained (739 mg, 1.57 mmol) were similarly decomplexed (120–140 °C, 22 Torr), giving 493 mg of TNF (100%) and 239 mg of colorless crystals (1.53 mmol). GC analysis showed that this material is 1 with high purity (99.91 wt %) containing a trace amount of 2 (0.09 wt %). Other DMN isomers could not be detected.

Determination of Association Constants (K_{CT}). In the presence of a large excess of DMNs, K_{CT} values for 1–TNF and 2–TNF were determined photospectroscopically in CH_2Cl_2 by using the Benesi–Hildebrand equation.[12] In these measurements, the concentration of TNF was $(1.26–4.42) \times 10^{-4}$ mol dm^{-3}, and those of DMNs were in the range of $(4.43 \times 10^{-2}) – 0.510$ mol dm^{-3}. CT absorption bands appeared as a shoulder in the 460–470-nm region, and linear correlations were observed by assuming a 1:1 molar ratio for both complexes. K_{CT} values for 1–TNF (ϵ at 470 nm, 1900 mol^{-1} dm^3 cm^{-1}) are 2.8, 1.8, and 1.3 mol^{-1} dm^3 at 0, 15, and 30 °C, respectively, and ΔH of −4.1 ± 0.1 kcal mol^{-1} was deduced from these values. In the case of 2–TNF (ϵ at 470 nm, 1400 mol^{-1} dm^3 cm^{-1}), K_{CT} are 2.8, 1.9, and 1.3 mol^{-1} dm^3 at 0, 20, and 30 °C, respectively, and ΔH is −4.0 ± 0.1 kcal mol^{-1}.

Preparation of CT Crystals 3 and 4. The powder sample of 3 was obtained in 59% yield by mixing 1 and TNF in CH_2Cl_2, mp 156–157 °C; IR (KBr) 1734 (C=O) cm^{-1} (1733 cm^{-1} for TNF itself).

Anal. Calcd for $C_{25}H_{17}N_3O_7$: C, 63.69; H, 3.63; N, 8.91. Found: C, 63.59; H, 3.49, N, 8.87.

An orange powder of 4 was also obtained by the direct method in CH_2Cl_2 in 47% yield, mp 141–143 °C; IR (KBr) 1735 (C=O) cm^{-1}.

Anal. Calcd for $C_{25}H_{17}N_3O_7$: C, 63.69; H, 3.63; N, 8.91. Found: C, 63.94; H, 3.41, N, 8.91.

X-ray Structural Analyses. An orange plate-like crystal of 3 with dimensions of 0.2 × 0.25 × 0.15 mm was obtained by slow evaporation of CH_2Cl_2 and used for the data collection. By using graphite monochromated Mo Kα radiation (λ = 0.710 49 Å) on an AFC-5R automated four-circle diffractometer with a rotating anode (180 mA, 45 kV), a total of 3823 independent reflections within $2\theta = 50°$ were collected at 13 °C. Crystal data are as follows: MF $C_{25}H_{17}N_3O_7$, MW 471.43, triclinic, $P\bar{1}$, a = 13.114 (3) Å, b = 10.066 (2) Å, c = 9.135 (2) Å, α = 72.64 (1)°, β = 76.08 (1)°, γ = 99.66 (2)°, V = 1079.1 (4) Å^3, Z = 2, and D_c = 1.451 g cm^{-3}. The structure was solved by the direct method using the RANTAN81 program[13] with some difficulty, and the space group was assumed to be noncentrosymmetric $P1$. After two kinds of molecules of 1 and one pair of TNF molecules had appeared in the E-map, it was proven that each of the DMN molecules lay on an inversion center and that two TNF molecules were related by a center of symmetry. After anisotropic refinement of non-hydrogen atoms in the space group of $P\bar{1}$ by the block-diagonal least-squares method, the positional parameters of the hydrogen atoms were calculated geometrically. They were included in the refinement at the final stage with isotropic temperature factors. No absorption correction was applied (μ = 1.012 cm^{-1}). The final R value is 7.34% for 2448 reflections with $|F_o| > 3\sigma|F_o|$. The final difference Fourier synthesis gave the largest peak of 0.35 e/Å^3. All calculations were carried out on an ACOS 2020 computer at Tohoku University using applied library programs of UNICS III system.[14]

An orange plate-like crystal (0.2 × 0.25 × 0.15 mm) of 4 was grown from benzene, and the data collection was similarly carried out (AFC-5R, 200 mA, 45 kV; Mo Kα, $2\theta < 55°$, 4284 independent reflections, at 13 °C). Crystal data are as follows: MF $C_{25}H_{17}N_3O_7$, MF 471.43, triclinic, $P\bar{1}$, a = 15.029 (2) Å, b = 10.650 (1) Å, c = 7.022 (1) Å, α = 77.21 (1)°, β = 93.11 (1)°, γ = 84.46 (2)°, V = 1087.5 (3) Å^3, Z = 2, and D_c = 1.440 g cm^{-3}. The structure was solved by the direct method (RANTAN81), and non-hydrogen atoms were refined with anisotropic temperature factors. The positional parameters of hydrogen atoms were calculated geometrically and included in the refinement. The final R value is 9.61% for 2384 reflections with $|F_o| > 3\sigma|F_o|$. The final difference Fourier synthesis gave the largest peak of 0.29 e/Å^3.

Measurement of Redox Potentials. Reduction potentials (E^{red}) of TNF and oxidation potentials (E^{ox}) of 1 and 2 were measured by cyclic voltammetry in dry MeCN containing 0.1 mol dm^{-3} Et_4NClO_4 as a supporting electrolyte. All the values shown in the text are in E/V vs SCE, and Pt wire was used as the working electrode. TNF underwent reversible three-stage one-electron reductions, and only the first reduction potential is shown. Voltammograms of 1 and 2 showed irreversible waves so that half-wave potentials were estimated from the anodic peak potentials (E^{pa}) as $E^{ox} = E^{pa} - 0.03$ V.

Supplementary Material Available: Listings of positional and thermal parameters and bond lengths and angles for 3 and 4 (6 pages). This material is contained in many libraries on microfiche, immediately follows this articles in the microfilm version of the journal, and can be ordered from the ACS; see any current masthead page for ordering information.

(12) Benesi, H. A.; Hildebrand, J. H. *J. Am. Chem. Soc.* **1960**, *82*, 2134.

(13) Jia-xing, Y. *Acta Crystallogr. Sect. A* **1981**, *37*, 642; **1983**, *39*, 35.

(14) Sakurai, T.; Kobayashi, K. *Rikagaku Kenkyusho Hokoku* **1979**, *55*, 69.